FOSSIL ENERGY

DOE/BC/15119-1
(OSTI ID: 789030)

QUANTITATIVE METHODS FOR RESERVOIR CHARACTERIZATION AND IMPROVED RECOVERY APPLICATION TO HEAVY OIL SANDS

Annual Report
October 1, 1998-September 30, 1999

By:
James W. Castle
Fred J. Molz

Date Published: November 2001

Work Performed Under Contract No. DE-AC26-98BC15119

Clemson University
Clemson, South Carolina

National Energy Technology Laboratory
National Petroleum Technology Office
U.S. DEPARTMENT OF ENERGY
Tulsa, Oklahoma

DOE/BC/15119-1
Distribution Category UC-122

Quantitative Methods for Reservoir Characterization and Improved Recovery Application to Heavy Oil Sands

By
James W. Castle
Fred J. Molz

November 2001

Work Performed Under DE-AC26-98BC15119

Prepared for
U.S. Department of Energy
Assistant Secretary for Fossil Energy

Ginny Weyland, Project Manager
National Petroleum Technology Office
P.O. Box 3628
Tulsa, OK 74101

Prepared by
Clemson University
300 Brackett Hall
Box 345702
Clemson, SC 29634

Table of Contents

Introduction

Improved prediction of interwell reservoir heterogeneity is needed to improve productivity and to reduce recovery cost for California's heavy oil sands, which contain approximately 2.3 billion barrels of remaining reserves in the Temblor Formation and in other formations of the San Joaquin Valley. This investigation involves application of advanced analytical property-distribution methods conditioned to continuous outcrop control for improved reservoir characterization and simulation. The proposed investigation is being performed in collaboration with Chevron Production Company U.S.A. as an industrial partner, and incorporates data from the Temblor Formation in Chevron's West Coalinga Field.

The first twelve months of the project have focused on collecting data for characterization and modeling. In addition, data from Coalinga Field has been analyzed to define the fractal structure present in the data set.

The following sections of the report parallel the first four subtasks of the investigation.

Collect and Load Property Data from Temblor Outcrops in California

The purpose of this phase of the investigation is to determine vertical and lateral facies variations within the Temblor Formation in order to identify correlative surfaces and to interpret depositional environments. Detailed investigation of outcrop exposures of the Temblor Formation on the Coalinga Anticline was conducted during May and June. Twelve vertical sections were measured, and the sedimentary features were described in detail. The exposures logged were selected to provide information on vertical and lateral variations within the Temblor Formation. The majority of the exposures studied are located in close proximity within sections 20 and 21, T19S, R15E (Domengine Ranch 7.5' quadrangle). The exposures studied are listed in Table 1. Approximately 2300 feet of vertical section were measured and described.

Sedimentological description of the exposures included logging of grain size, percent sand, biogenic features, and sedimentary structures. Complete gamma-ray profiles were recorded for each section using a hand-held scintillometer. Gamma-ray values were recorded at 0.5-foot intervals. All gamma-ray data have been loaded into a digital database. Digital photo-mosaics of the exposures were made.

Based on study of the Temblor Formation exposures, two major transgressive-regressive cycles are recognized in the formation. A thick lower interval of sand represents deposition on an unconformable surface that was incised during lowstand of relative sea level. This surface represents approximately 15 million years of non-deposition, during which time substantial erosion of the underlying Kreyenhagen Shale occurred in some areas. Valleys incised into the Kreyenhagen Shale were filled during subsequent rise of relative sea level, which produced a succession of stacked fining-upward sequences. The fining upward sequences typically contain basal, trough cross-bedded cobbles and pebbles above a scoured contact. Grain size decreases upward through coarse- and medium-grained sand to silt and then clay. Marine influence in this valley-fill succession, which reaches a thickness of approximately 45 m, increases upward through estuarine deposits and into marine clay. Clay beds contain sparse

burrows, which are clay lined and sand filled. Regressive deposits of a tide-dominated shoreline overlie the incised-valley transgressive systems tract. The regressive accumulation, which becomes coarser grained upward, consists of alternating tidal-channel and intertidal-flat deposits. These sediments contain ripple cross lamination, clay drapes, and finely interlaminated silt, sand, and clay. Sand beds containing abundant shell debris separate depositional cycles and serve as useful marker horizons within this interval. Several distinctive types of shell beds were recognized, including oyster beds, barnacle beds, and debris beds containing shell fragments of clams, gastropods, mollusks, and ammonites. The regressive tidal-shoreline deposits are capped by a diatomite bed, up to 9 m thick, that represents deposition in response to relative rise in sea level. In the upper part of the Temblor Formation, a regressive tidal and coastal-plain succession of sand and clay overlies the diatomite.

The results of this part of the investigation were presented at the annual national meeting of the Geological Society of America in October (Bridges et al., 1999).

Collect and Load Property Data from Temblor Reservoir Sands, West Coalinga Field, California

The collection and loading of property data from Temblor reservoir sands in West Coalinga Field focused on two phases:

1) Detailed description of cores and comparison to geophysical logs; and
2) Quality control and loading of digital core-analysis data.

Both phases were completed in close collaboration with Chevron, with Chevron providing core-analysis data, core descriptions produced by their geologists, use of core photographs, facilities for core examination, and manpower support for core layout and preparation.

Approximately 4470 feet of cores from 13 wells in Coalinga Field were described by Clemson University personnel during the summer (Table 2). Description included logging the same features and using the same format as followed for the outcrop work. Grain size, percent sand, biogenic features, and sedimentary structures were logged. In addition, notations of Chevron's facies classification and degree of oil staining were recorded. In order to facilitate integration of outcrop results with subsurface information from Coalinga Field, five of the thirteen cores described are from the northern part of the oil field, which is nearest to the surface exposures. All of the cores were provided by Chevron, and the work was preformed at the Chevron Geologic Warehouse in Richmond, California.

Working cooperatively with Chevron personnel, core-analysis (i.e., porosity and permeability) data were loaded into a digital database (Excel spreadsheets). Prior to loading, data were examined for quality control, and depths were adjusted to match geophysical logs. Quality control work was done by Chevron personnel and by Clemson personnel working closely with Chevron. All wells with cores described and core-analysis data are listed in Table 3.

Collect and Load Property Data from Continuous Upper Cretaceous Outcrops in Utah

Geological Data

The purpose of this phase of the investigation is to obtain information that will contribute to developing a geologically realistic outcrop-conditioned model for application to characterizing heavy-oil sands in Coalinga Field. Fifteen stratigraphic sections in the A Sandstone (middle portion of the John Henry Member of the Upper Cretaceous Straight Cliffs Formation) were measured and described in the vicinity of Escalante, Utah. A total of 1,150 feet of section were studied in detail. Sedimentological description of the exposures included logging of grain size, percent sand, biogenic features, and sedimentary structures. Gamma-ray profiles of each section were recorded using a hand-held scintillometer. All gamma-ray data have been loaded into a digital database.

The majority of sections are in the upper part of the A Sandstone and above the A sequence boundary (as defined by Hettinger et al., 1993). Five of the sections logged include the lower part of the A sandstone, which is beneath the A sequence boundary. Eleven sections are approximately parallel to depositional strike, while the remaining four sections follow depositional dip. Seven closely spaced strike sections were described for the purpose of determining small-scale geological variability.

Based on the vertical sequences of texture and sedimentary structures, the most common depositional environments represented are estuarine and tidal. The following features indicate tidal influence: bi-directional cross-bedding, reactivation surfaces, mud drapes, and mud couplets. Variable energy levels are indicated by alternating beds of cross-bedded facies and bioturbated facies, with the cross-bedded facies indicating higher energy than the bioturbated facies.

Due to the long, continuous nature of the outcrops, it is possible to trace units between most of the logged sections. In particular, resistant beds of well cemented, cross-bedded sandstone encased within bioturbated facies can be traced readily. These resistant units, which are approximately 1 to 5 feet thick, contain horizontal bedding, low-angle cross-bedding, and trough cross-bedding. These beds are likely to be significant in the distribution of flow properties.

New Field Method for Permeability Measurement

In early May of this year, several specific sites in the field area near Escalante, Utah were identified for permeability measurement. Part of the study was experimental in nature in that a large number of air permeability measurements were planned. By the middle of June, equipment was in place at a selected site, and we began to collect small core plugs so that air permeability measurements could be made in the laboratory. It was necessary to perform measurements on the internal end of core plugs, because recent data (Forster, 1999) show that weathering processes alter the rock surface such that surface-measured permeabilities are not representative of the true, unweathered permeability distribution located a few inches below the exposed surface.

It soon became apparent that the Utah rock exposures, composed mostly of tidal and estuarine sandstones, could not be cored without doing extensive damage to the cores. This was due to the fact that the rock was often weakly cemented and contained a large fraction of fine-grained sediment. This sediment formed a muddy material when mixed with coring fluid (water), and the resulting slurry abraded the cores that we were attempting to retrieve. It was decided to try air as a coring fluid. However, this failed also, because with air the core vibrated violently within the core barrel and became pulverized. We finally concluded that coring was not practical in the Utah rock outcrops, at least not from a permeability-measurement viewpoint.

In the process of studying the problem, it was observed that while minimally disturbed cores could not be collected successfully, it was very easy to drill small, high quality holes in the outcrops using a simple masonry drill. It was reasoned that if we could make permeability measurements at the bottom of such holes, a high quality data set would result. Unfortunately, an air permeability probe for making such measurements is not available, and the theory for analyzing radial airflow from a cylindrical hole has not been developed. Probe and theory exist only for surface-applied flow. It was concluded that in order for our planned measurements to be successful, it would be necessary to develop a small cylindrical permeameter probe that could be inserted and sealed in a small drill hole, and also the necessary theory to calculate intrinsic permeability from injection pressure and mass flow rate measurements. When this conclusion was reached, field permeability measurements were postponed, and work on the new methodology began. When the new instrumentation and analytical techniques are available, we plan to return to Utah, probably in the late spring or early summer of 2000, and complete the permeability measurements. One of the advantages of the new technology is that it will be a true field method that can be applied manually, unlike the existing technology which is sold as a field method, but actually requires a laboratory environment to produce realistic permeability values.

We have been working on the new methodology since mid-June, and excellent progress has been made. Two types of prototype permeability probes have been designed and constructed: the seal of one type operates via tension, and the seal of the other type operates via compression. Use of the new probes prescribes a change in the system geometry. It was necessary to derive the mathematical theory for this new type of probe in a way that is analogous to Goggin, Thrasher, and Lake's (1988) derivation for the probe that applies flow to an exposed rock surface. There is a geometric factor for our probe system, just as there was a geometric factor for the probe system of Goggin et al. (1988). This factor accounts for the geometry of the system and nonlinear flow through the system. In order to determine the geometric factor for the new probe, finite-difference computer simulations are in development to model the pressure-distribution throughout the system. We have advanced toward this by first verifying Goggin's finite-difference solutions for the probe that applies flow to an exposed rock surface. We are approaching the completion of this segment, at which point we will modify the boundary conditions of the simulation to reflect the new system geometry. Once we have determined the geometric factor for the new probe geometry, lab testing can commence.

Several sandstone boulders from the field site in southern Utah have been transported to Clemson University for testing of the new prototype permeability probes.

Laboratory testing of the prototypes in the field-site sandstone will facilitate the move to *in situ* measurements in southern Utah in the late spring or early summer of 2000.

A paper on development of the new field permeameter probe will be presented at the national fall meeting of the American Geophysical Union (Dinwiddie et al., 1999).

Define Fractal Structure in the Data Sets and Apply to Generating Property Representations

Introduction

During the first twelve months of the project, techniques were identified for applying multi-scaling (multifractal) concepts to permeability (k) distributions in cores from West Coalinga Field. Spectral analyses and the Double Trace Moment (DTM) method (Lavallee et al., 1991) were used to analyze the scaling and multifractality of the permeability data. This was done by estimating the parameters of the Universal Multifractal (UM) model (Schertzer and Lovejoy, 1987). The UM model has been successful in representing, among other geophysical fields, spatial distribution of rain (Schertzer and Lovejoy, 1987), ice core formation structures (Schmitt et al., 1995), and topography (Lavallee et al., 1993). Papers by Gupta and Waymire (1993) and Veneziano (1999) provide additional useful information regarding multifractal models.

Data Analysis

Permeability data from five wells were used for the analysis. The vertical spacing of measurements was generally about 0.3048 m (one foot). Due to missing measurements, only portions of the data could be used (246 values out of about 1,000 values). Two disjoint data sets were obtained from Well 4: Well 4A and Well 4B. Figure 1 shows plots of the intrinsic permeability as a function of depth for all wells.

Figure 2 shows that scaling exists in the permeability field. The slope T ranged generally from about –1.05 to about –1.35, with an arithmetic average of about –1.2. This is not too far from the limiting stationary value of –1.

Although the DTM method has been restricted previously to stationary data sets, the plots in Figure 2 show that such a limitation is not necessary. One can transform the non-stationary data to stationary data by performing a fractional differentiation (which can be easily done in the Fourier space by multiplication by f raised to a positive power) to bring the slope T between –1 and +1. Consider for example Well 3, the slope T is equal to –1.17, hence it suffices to multiply (in Fourier space) the Fourier transforms of the measured k values by $f^{0.085}$ to obtain a new slope T = -1 (because the spectrum is the square of the Fourier transform magnitude). Alternatively, one can obtain stationary data by taking the increments of the data in the real space, which corresponds to a multiplication by f in the Fourier space (Lavallee et al., 1993). This is the approach followed in our work. We then took the absolute values of the increments, which is a necessary step for application of the DTM method (which requires a nonnegative field F).

The resulting field F is generally different from φ, which can be obtained only after α and σ are found.

We now proceed to estimating the parameters α and σ using the DTM method applied on the field F. Ideally, the scale ratio λm is the number of available data points in each well log and λi should vary from λm to 1. However, due to the fact that the standard DTM method relies on coarse-graining by increments that are a power of 2, we consider for each well a data length of 2^n, where n is the largest positive integer such that $2^n < \lambda m$. In cases where a large amount of data had to be discarded (for example Well 4B had 49 points, hence utilizing $2^5 = 32$ points results in 17 points being discarded), we applied the DTM method separately to the first 2^n points of the data and then to the second 2^n points of the data.

We computed DTM_q, using equations representing the scaling of the double trace moments, for η varying from 0.1 to 2.0 and for q=0.5 and 2.0. The plots in Figures 3 and 4 show the DTM_q for q=0.5 and q=2 for Wells 4B (first part) and Well 5 for selected η values. Notice that the linear fit is generally good in all graphs, indicating that multiscaling (or multifractal behavior) is obeyed. A break in scaling occurred for Well 5 at low λ values (Fig. 4). This was probably because of the combined effect of limited data length and intermittency (Fig. 1F), which resulted in spatial averages (using the equations representing the scaling of the double trace moments) being poor estimates of ensemble averages at low λ (notice that only one value is used for λ=1). This occurred to a lesser extent for other wells probably because of their lower degree of intermittency in comparison to Well 5 (Fig. 1). The fact that such a break was not observed for Well 2 (whose data are highly intermittent) could well be a fortunate event. Further investigation of this issue is left for future work.

Figure 5 shows plots of $\text{Log}|M(q, \eta)|$ versus η and the best-fit linear curve for Wells 4B (first part) and Well 5. The break in the linear behavior at high η values is expected because of the divergence of the dressed moments (Schertzer and Lovejoy, 1991).

Table 4 lists the estimated α and σ values from various data sets. The parameter α varied between 1.57 and 1.93 while σ varied between 0.042 and 0.43. The arithmetic averages of α and σ (obtained by averaging within each data set and then averaging between sets) were about 1.78 and 0.17, respectively.

Both parameters were quasi-constant for each data set independently of the order of moment, q. The difference between the first part of the data of Wells 1, 2, 3, and 4B is probably due to sampling. The same can be said for the difference between the estimates obtained from Well 4 (Well 4A and 4B).

From the observed spectral slopes (Fig. 2) and the values of α and σ for each data set (Table 4), we computed values of Hm varying between 0.19 and 0.32, with an average value of about 0.25.

Summary

Spectral analyses and the Double Trace Moment method (Lavallee et al., 1991) were used to analyze the scaling and multifractality of permeability data from cores from Coalinga Field. This was accomplished by estimating the parameters of the Universal

Multifractal (UM) model (Schertzer and Lovejoy, 1987). The UM parameters α (the multifractality parameter and the Levy index), σ (the codimension of the mean field and the width parameter of the Levy distribution), and Hm (the stationarity parameters) were estimated at 1.78, 0.17, and 0.25, respectively. One-dimensional and 2-D isotropic K fields were generated following the procedure of Wilson et al. (1991) and Pecknold et al. (1993), and 2-D anisotropic fields were generated according to a empirical procedure that was developed. The results of this work indicate the presence of fractal scaling in the permeability data from West Coalinga Field.

References

Forster, C.B., University of Utah, Dept. of Geology & Geophysics, Personal Communication, May 5, 1999.

Goggin, D.J., Thrasher, R.L., and Lake, L.W.: Experimental Analysis of Minipermeameter Response Including Gas Slippage and High Velocity Flow Effects," University of Texas at Austin, July 1988.

Gupta, V. K., and E. Waymire, A statistical analysis of mesoscale rainfall as a random cascade, *J. Appl. Meteorol.*, 32, 251-267, 1993.

Hettinger, R.D., P.J. McCabe, and K.W. Shanley, Detailed facies anatomy of transgressive and highstand systems tracts from the Upper Cretaceous of southern Utah, in: P. Weimer and H. Posamentier (ed.), *Siliciclastic Sequence Stratigraphy*, American Association of Petroleum Geologists Memoir 58, p. 235-257, 1993.

Lavallee, D., D., Schertzer, and S. Lovejoy, On the determination of the codimension function, in Nonlinear Variability in Geophysics, Editors: D. Schertzer and S. Lovejoy, 41- 82, Kluwer Academcis Publishers, the Netherlands, 1991.

Lavallee, D., S. Lovejoy, D. Schertzer, and P. Ladoy, Nonlinear variability and landscape topography: Analysis and simulation, in Fractals in Geography, Editor L. De Cola and N. Lam, Prentice Hall, 158-192, 1993.

Pecknold, S., S. Lovejoy, D. Schertzer, C. Hooge, and J. F. Malouin, The simulation of universal multifractals, in *Prospects in Astronony and Astrophysics*, Editor JM Perdand and A. Lejeune, Cellular Automata, 228-267, 1993.

Schertzer, D., and S. Lovejoy, Physical modeling and analysis of rain and clouds by anisotropic scaling multiplicative processes, *J. Geophys. Res.*, 92, 9693-9714, 1987.

Schertzer, D., and S. Lovejoy, Nonlinear geodynamical variability: Multiple singularities, universality, and observables, in *Nonlinear Variability in Geophysics*, Editors: D. Schertzer and S. Lovejoy, 41- 82, Kluwer Academic Publishers, the Netherlands, 1991.

Schmitt, F., S. Lovejoy, and D. Schertzer, Multifractal analysis of the Greenland ice-core project climate data, *Geophys. Res. Let.*, 22, 1689-1692, 1995.

Veneziano, D., Basic properties and characterization of stochastically self-similar processes in R^d, *Fractals*, 1999, in press.

Wilson, J, D. Schertzer, and S. Lovejoy, Continuous multiplicative cascade models of rain and clouds, in *Nonlinear Variability in Geophysics*, Editors Daniel Schertzer and Shaun Lovejoy, Kluwer Academics Publishers, the Netherland, 185-207, 1991.

Published Abstracts/Presentations of Results

Bridges, R. A., Castle, J. W., and Clark, M. S., Depositional Patterns and Sequence Stratigraphy of the Miocene Temblor Formation, San Joaquin Basin, California: Geological Society of America Abstracts with Programs, October 1999.

Dinwiddie, C. L., Molz, F. J., Murdoch, L. C., and Castle, J. W., A New Mini-Permeameter Probe and Associated Analytical Techniques for Measuring the *In Situ* Spatial Distribution of Permeability: American Geophysical Union, 1999 Fall Meeting, 1999, in press.

Table 1. Outcrop localities of the Temblor Formation studied near Coalinga Field. The thickness logged at each location is listed.

Locality	Stratigraphic Interval	Location – UTM	Location – Section, Township, Range	Feet
Cartwheel Ridge	Temblor	4015500mN/ 737500mE	SEC. 20, T19S, R15E	505
Razorback Ridge	lower Temblor	4015200mN/ 737550mE	SEC. 20, T19S, R15E	229
Side Cliff of Laval Grade	middle Temblor	4015250mN/ 737570mE	SEC. 20, T19S, R15E	41
Laval Grade 1 with middle Gully Cut	Temblor to Diatomite	4016000mN/ 738000mE	SEC. 21, T19S, R15E	389
Laval Grade 2 with Southmost Gully Cut	Temblor to Diatomite	4015900mN/ 738000mE	SEC. 21, T19S, R15E	388
Laval Grade 3	middle Temblor	4016100mN/ 738000mE	SEC. 21, T19S, R15E	72
Shell Cut 1	lower Temblor	4016200mN/ 738150mE	SEC. 21, T19S, R15E	48
Shell Cut 2	lower Temblor	4016200mN/ 738150mE	SEC. 21, T19S, R15E	101
Shell Cut 3	lower Temblor to C-sand	4016150mN/ 738300mE	SEC. 21, T19S, R15E	292
Shell Cut 4	lower Temblor	4016200mN/ 738000mE	SEC. 21, T19S, R15E	61
Big Tar Canyon	middle and upper Temblor	3980000mN/ 755890mE	SEC. 18, T23S, R17E	110
North Gully Cut	lower Temblor	4016000mN/ 737850mE	SEC. 21, T19S, R15E	77
			TOTAL	2313

Table 2. Cores from West Coalinga Field that were described during summer 1999.

Well	Location (Section)	Feet
S6-3	31A	120
3-10A	13D	295
S3-5	31A	364
5-6T1	24D	320
3-5	7C	559
S7-3	31A	568
3-10	7C	570
118A	36D	185
6-3D	13D	421
S4-9	31A	259
10-6W	25D	191
2-9W	31A	230
8-2W	25D	385
	TOTAL	4,467

Table 3. Core descriptions and core-analysis data from West Coalinga Field. The cores described by Clemson University personnel are listed in Table 2. Chevron personnel described the remaining cores.

Well	Location (Section)	Core Analysis Data	Core Description
6-6a	12D	X	
S10-7	31A	X	
12-4A	12D	X	
3-5	7C	X	X
S3-5	31A	X	X
118A	36D	X	X
2-9W	31A	X	X
3-10A	13D	X	X
S-6-3	31A	X	X
S4-9	31A	X	X
3-10	7C	X	X
5-5W	31A		
1-7T1	31A		
6-3D	13D	X	X
11-5A	13D		
S7-3	31A		X
10-6W	25D		X
5-6T1	24D		X
8-2W	25D	X	X
132A	36D	X	X
258A	36D	X	X
9-1A	36D	X	X
5-7T1	25D	X	X
4-15	24D	X	
9-4T1	13D	X	X
WD-8	18C	X	X
57	18C	X	X
65	18C	X	X
6-11A	6C	X	X
2-10	6C	X	X

Table 4. Values of α and σ Estimated by the DTM method.
The average values are α=1.78 and σ=0.17

		q=0.5		q=2.0		
		α	σ	α	σ	Comment
Well 1	1st Part	1.80	0.137	1.81	0.159	16 out of 26 data points
	2nd Part	1.83	0.4323	1.75	0.4157	16 out of 26 data points
Well 2	1st Part	1.74	0.048	1.71	0.055	32 out of 55 data points
	2nd Part	1.72	0.146	1.61	0.132	32 out of 55 data points
Well 3	1st Part	1.93	0.047	1.84	0.042	16 out of 27 data points
	2nd Part	1.70	0.185	1.57	0.163	16 out of 27 data points
Well 4A	One Set	1.79	0.155	1.70	0.151	20 data points
Well 4B	1st Part	1.82	0.168	1.78	0.175	32 out of 49 data points
	2nd Part	1.90	0.172	1.90	0.186	32 out of 49 data points
Well 5	One Set	1.88	0.234	1.76	0.194	64 out of 67 data points

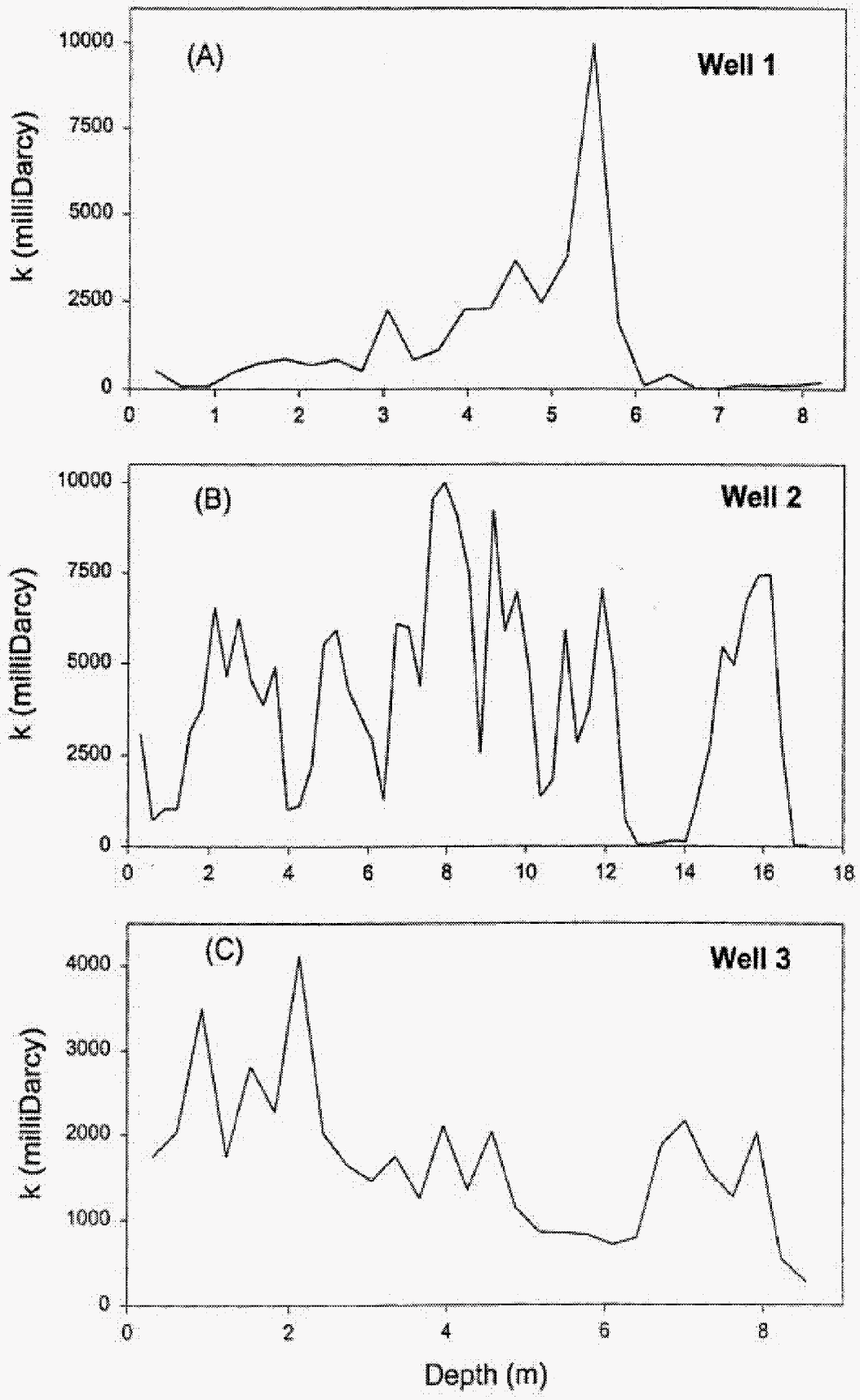

Figure 1. Observed permeability data from Coalinga Field, California.

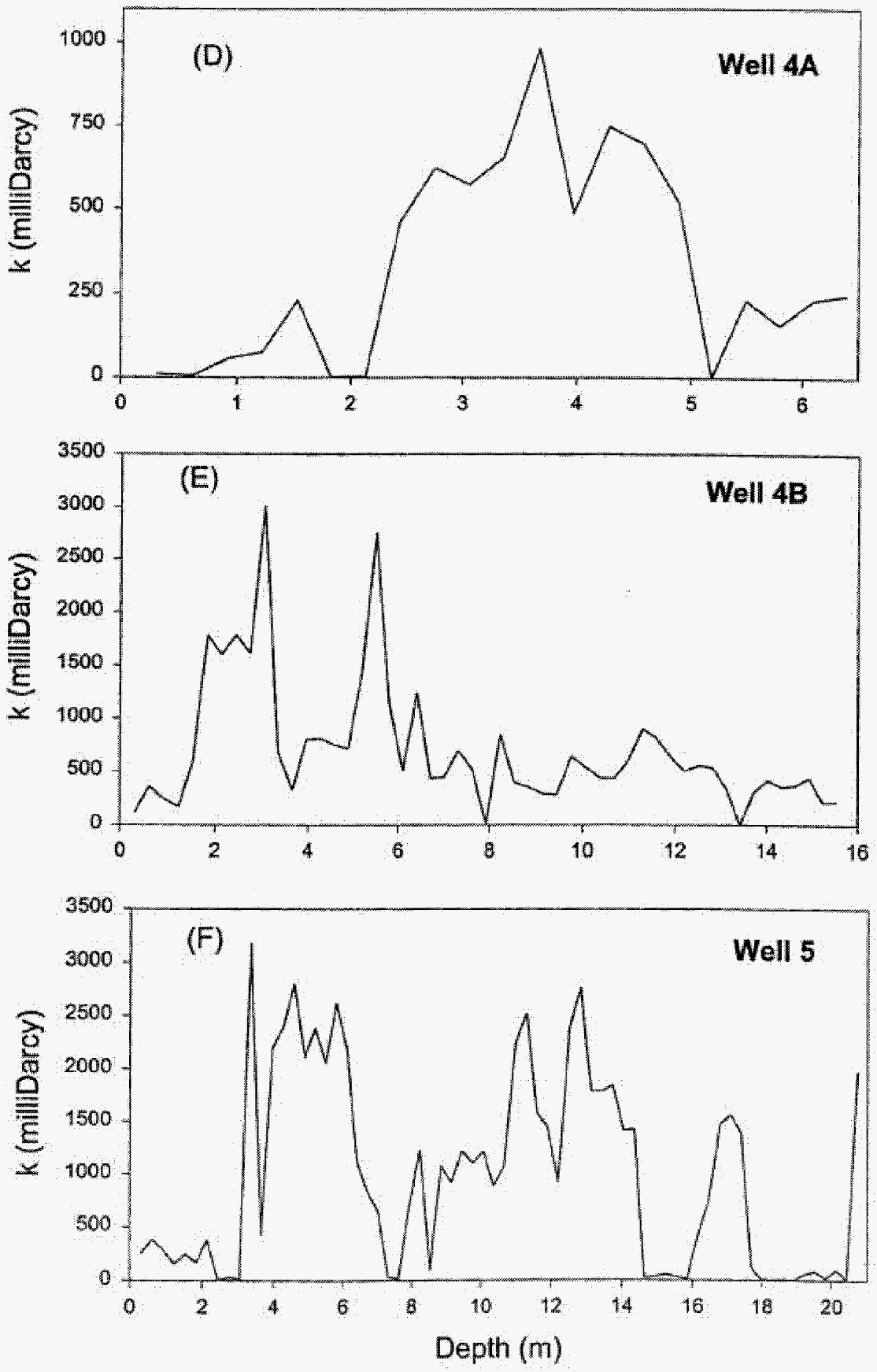

Figure 1. Continued

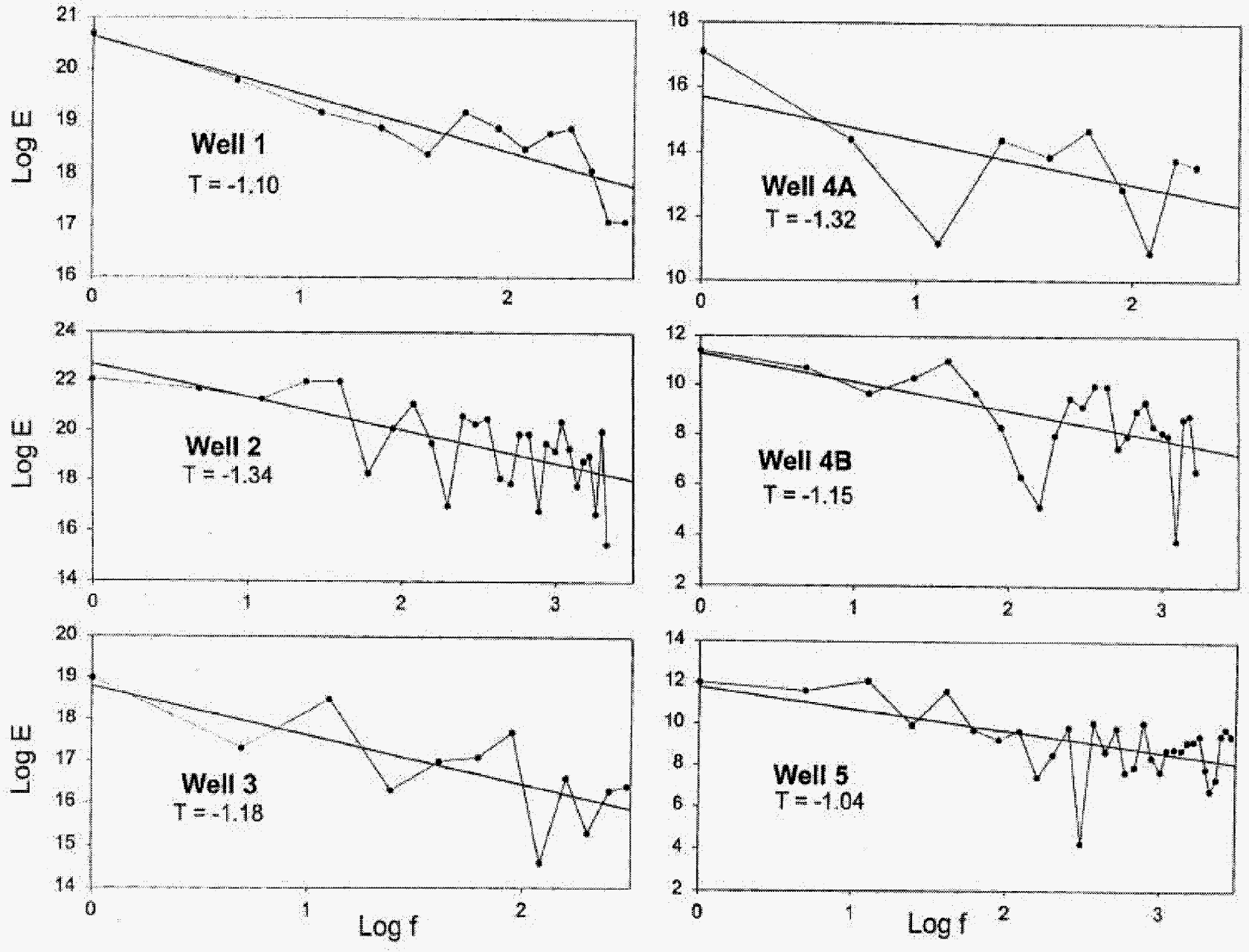

Figure 2. Observed spectral slopes of the permeability data reported in Figure 1.

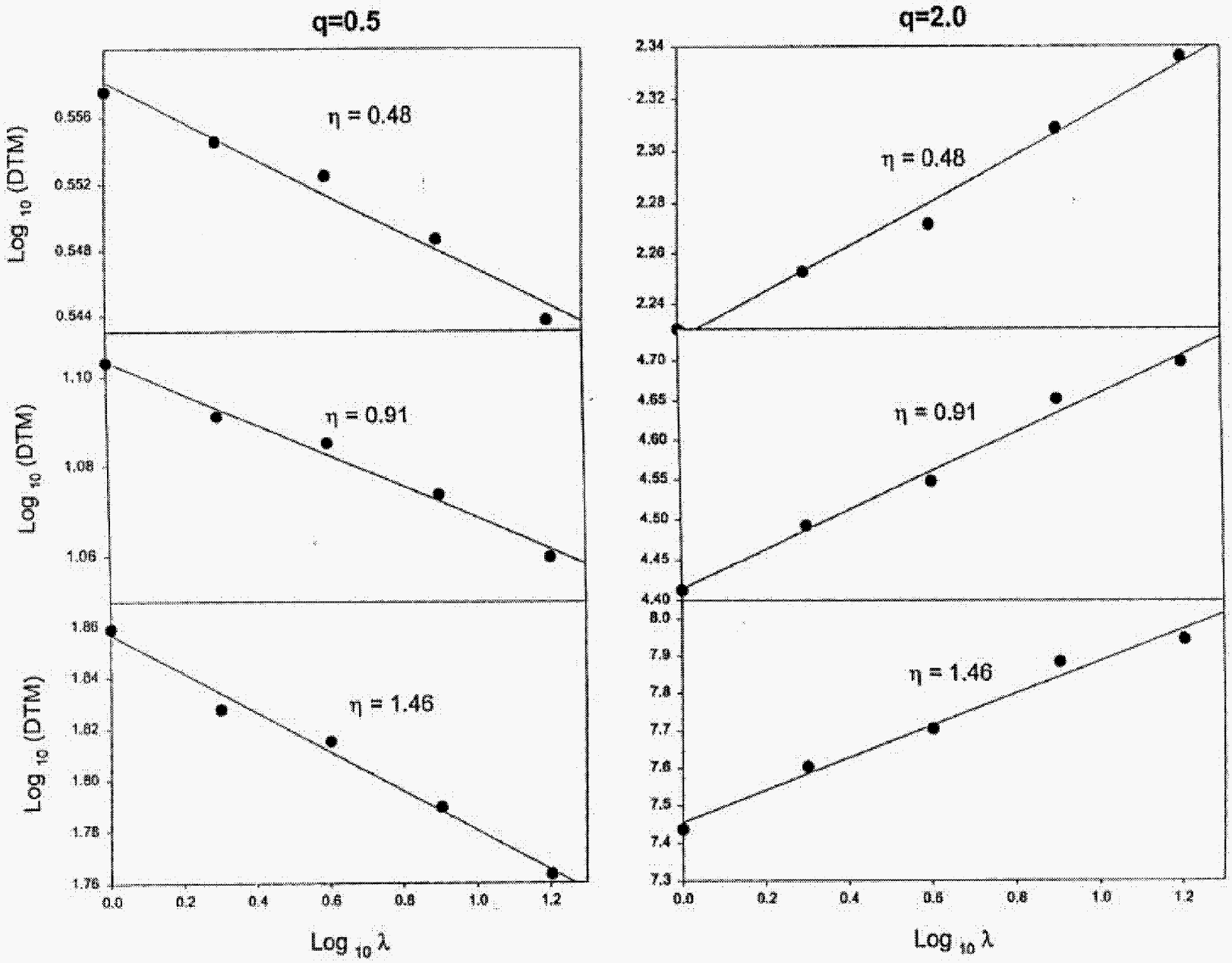

Figure 3. DTM (from equations representing the scaling of the double trace moments) for Well 4B (First Part).

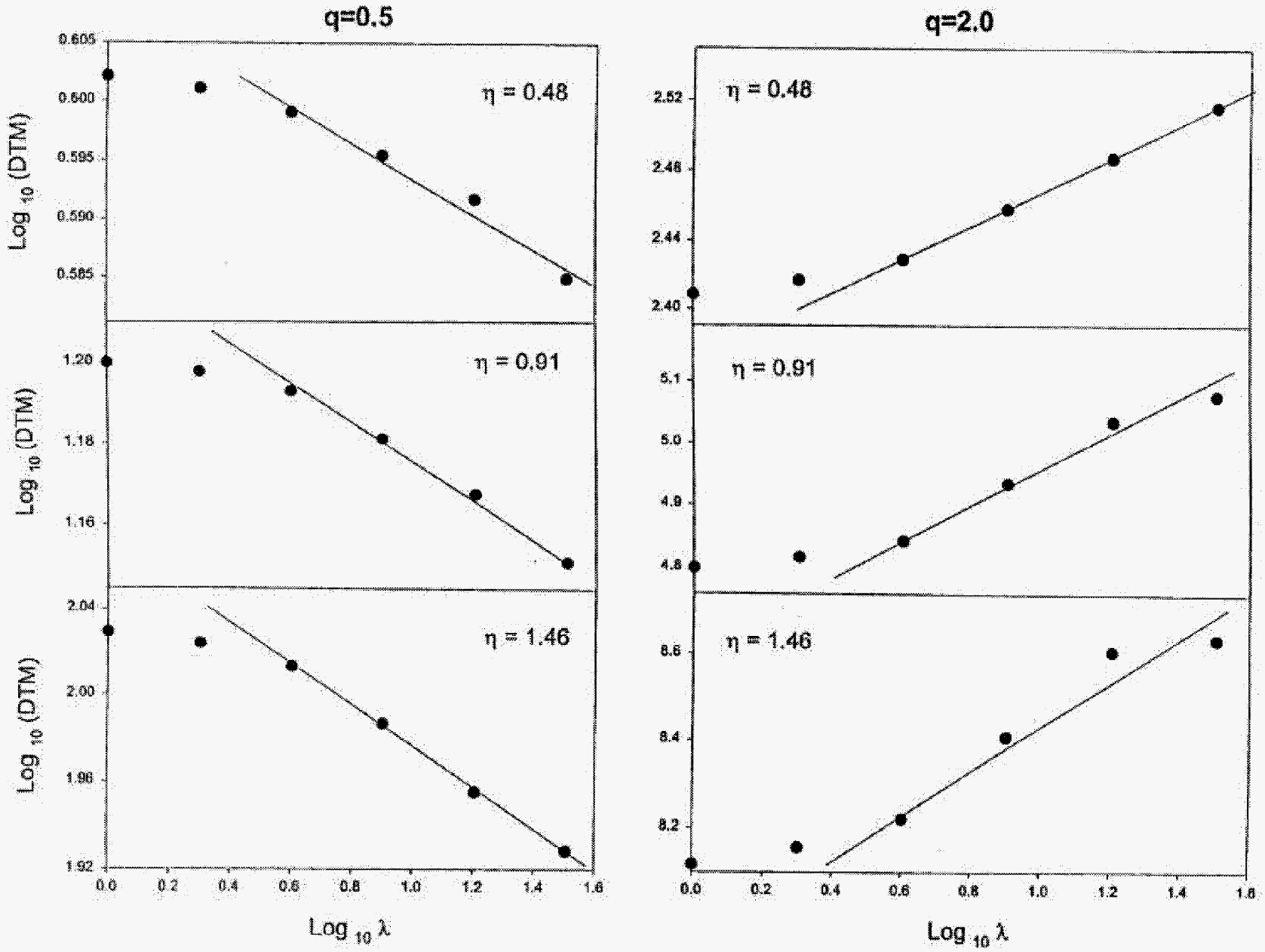

Figure 4. DTM (from equations representing the scaling of the double trace moments) for Well 5.

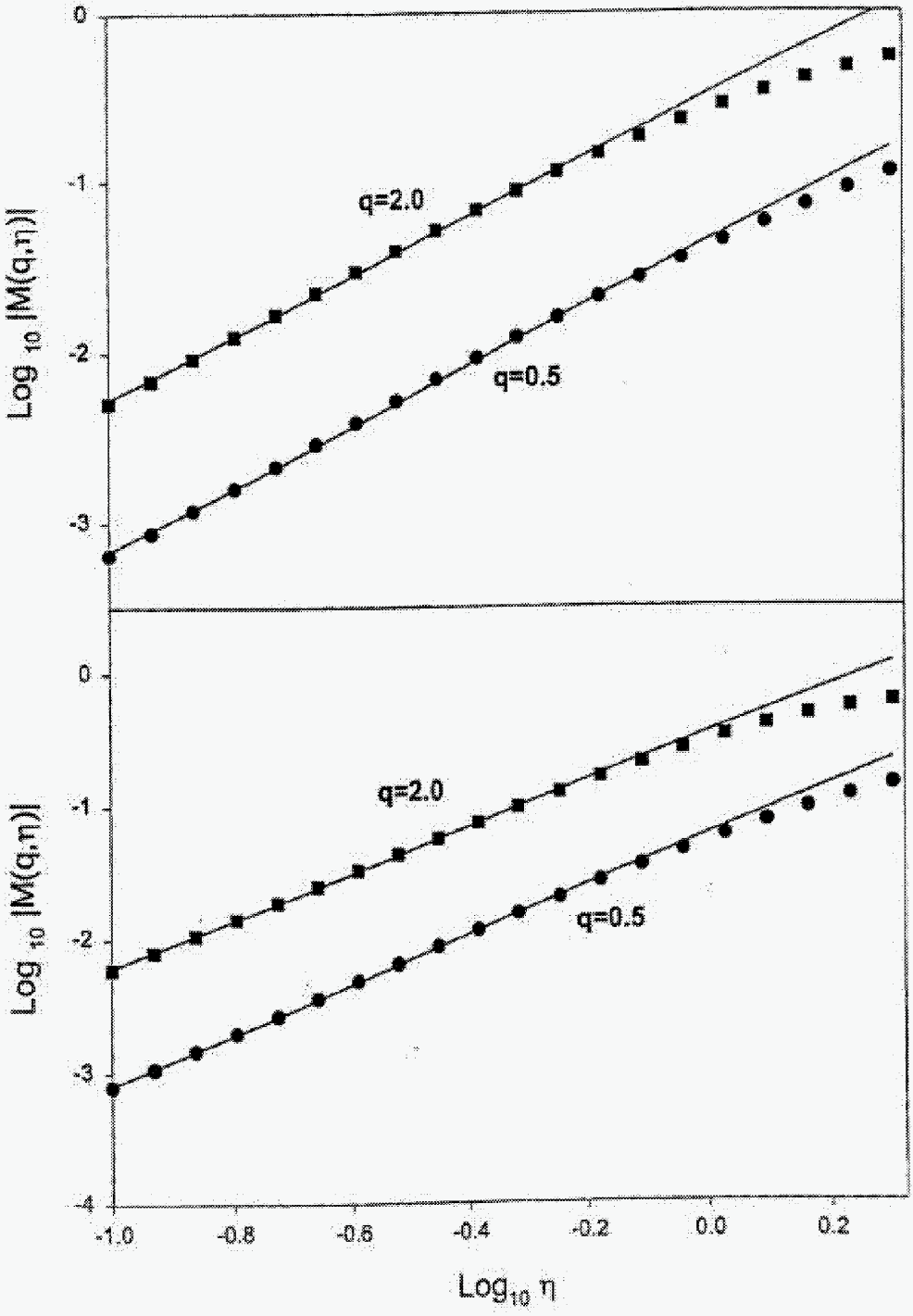

Figure 5. Log $|M(q,\eta)|$ as a function of Log η for A) Well 4B (First part) and B) Well 5. Note the goodness of fit at low η values.